JOURNAL OF THERMOPHYSICS AND HEAT TRANSFER
Vol. 9, No. 1, January–March 1995

Estimation of Excitation Energy of Diatomic Molecules in Expanding Nonequilibrium Flows

Chul Park*
NASA Ames Research Center, Moffett Field, California 94035

The energy contained in the highly excited vibrational and rotational states in a diatomic gas in a thermochemical nonequilibrium state during expansion is estimated. The population distribution of the vibrational and rotational states is assumed to be describable by a polynomial. The parameters in the polynomial are determined by invoking known physical constraints. The energy contained in the internal states in excess of that accounted for in the conventional method is calculated for N_2, O_2, NO, CO, and H_2. The calculation is carried over a wide range of conditions, and the results are fitted with polynomials. The population distributions so determined agree with the theoretical and experimental results of others. A sample calculation made for a typical nozzle flow shows that the excess energy may reach 6% of the total enthalpy of the flow, and that the flow velocity may decrease by 3% due to this phenomenon.

Nomenclature

A = cross-sectional area of nozzle
a_i = coefficients of expansion of ρ, Eq. (29)
c = continuum state
D = dissociation energy measured from the ground vibrational state, eV or cm^{-1}
E = combined vibrational-rotational energy ($E_v + E_r$), eV or cm^{-1}
$E(i)$ = energy level of state i, eV or cm^{-1}
E_r = rotational energy per molecule, eV or cm^{-1}
E_v = vibrational energy per molecule measured from the ground vibrational state, eV or cm^{-1}
E_x = excess vibrational-rotational energy per unit mass, J/kg, Eq. (3)
g = rotational statistical weight, $2J + 1$
H = enthalpy
i, i' = indices representing an internal state
J = rotational quantum number
$K(i, i')$ = rate coefficient for collisional transition from state i to state i', m^3/s
k = Boltzmann constant
M = see Eq. (8)
m = exponent in Eq. (29)
n = exponent in Eq. (29), or number density, m^{-3}
$n_E(i)$ = number density of state i in equilibrium, m^{-3}
$n(i)$ = number density of state i, m^{-3}
n_x = number density of colliding particles, m^{-3}
p = pressure, atm
Q = partition function
R = absolute radius in E_v vs E_r coordinate system, eV or cm^{-1}, Eq. (10)
r = normalized radius, Eq. (11)
T = heavy particle translational temperature, K
T_r = rotational temperature defined by lowest two states, K
T_v = vibrational temperature defined by lowest two states, K
t = time, s
V = flow velocity, m/s
v = vibrational quantum number
$\bar{v}$ = average thermal speed, m/s
α = kT/D
δT_r = see Eq. (16)
δT_v = see Eq. (13)
ε = vibrational-rotational energy, eV or cm^{-1}
Θ = characteristic vibrational temperature (ω_e/k), K
θ = polar angle in E_v vs E_r coordinate system, rad, Eq. (12)
$\rho(i)$ = normalized nonequilibrium population for state i, Eq. (5)
ρ_M = normalized nonequilibrium molecular density, Eq. (38)
$\bar{\rho}$ = fluid density, kg/m^3
σ = excitation cross section, m^2
ω_e = first vibrational constant, eV
$\omega_e x_e$ = second vibrational constant, eV

Subscripts
A = atomic species A
av = average energy
B = atomic species B
E = equilibrium
M = molecule
m = maximum value
s = settling chamber
0 = origin in E_v vs E_r coordinate system

Superscript
* = throat

Introduction

IT is known that the internal energy of a gas in a high-enthalpy, low-density flow may deviate from those expected under equilibrium conditions. To predict the aerodynamic and heating environments under such conditions, a multitemperature thermochemical nonequilibrium model has been developed in recent years (see Chap. 4 of Ref. 1). In that model, the energies contained in the internal modes of atoms or molecules, i.e., vibration, rotation, and electronic excitation, are calculated independently of the translational energy. The temperatures characterizing the internal energies are then deduced assuming that the internal states are populated according to a Boltzmann distribution.

Presented as Paper 92-0805 at the AIAA 30th Aerospace Sciences Meeting, Reno, NV, Jan. 6–9, 1992; received Jan. 14, 1994; revision received May 13, 1994; accepted for publication May 17, 1994.
*Staff Scientist. Associate Fellow AIAA.

Under the assumption of a Boltzmann distribution and a rigid rotator, the rotational temperature is related to rotational energy by

$$E_r = kT_r, \quad \text{eV} \tag{1}$$

For the vibrational mode, it is customary to assume that all vibrational energies are contained in the ground electronic state and that molecules behave as a harmonic oscillator, which leads to

$$E_v = \frac{k\Theta}{\exp(\Theta/T_v) - 1}, \quad \text{eV} \tag{2}$$

In a compressive nonequilibrium region, such as behind a normal shock wave in which dissociation and ionization occur, the upper states of the internal modes are generally underpopulated while the chemical reactions are in progress, i.e., attain number densities smaller than those dictated by the Boltzmann relation. By assuming the internal states to be populated according to a Boltzmann distribution, the internal energy is overestimated. Since the upper state contribution is small even in a Boltzmann distribution, this error is usually negligibly small.

When a molecular species is heated to a dissociating temperature in a settling chamber, and is expanded through a nozzle, an atomic recombination process occurs in the nozzle. The ensuing coupled vibration-recombination nonequilibrium relaxation process has been a subject of an intensive study in the past three decades.[2-21] It became known, both through theoretical reasoning[2-7,12,13] and experimental verification,[14-16] that the low intermediate vibrational levels tend to acquire a concave-upward population distribution known as Treanor distribution, due to the prevelance of the vibration-to-vibration energy exchange and anharmonicity of the vibrational energy levels. The uppermost vibrational levels tend to be in equilibrium with the free (dissociated) states,[9-11] and hence, are generally overpopulated in relation to the lower vibrational states.

These overpopulated upper vibrational states contain energy not accounted for by Eq. (2). A similar phenomenon exists for the rotational mode. Expressing the average excitation energy by ε, the excess energy per unit mass can be defined by

$$E_v = n_M \left[\varepsilon - kT_r - \frac{k\Theta}{\exp(\Theta/T_v) - 1} \right] \Big/ \bar{\rho}, \quad \text{J/kg} \tag{3}$$

This excess energy can potentially be sufficiently large to be of concern. By ignoring this excess energy, one errs in determining the state variables. One consequence of this will be that the flow velocity may be overestimated. This would lead to overestimation of thrust in rocket engines, and of forces acting on a model placed in a wind tunnel.

The existing theoretical works on the distribution of high vibrational states[9,10] show considerable variation. This is partly because of the uncertainties in interaction potentials in calculating the state-to-state vibrational transition rates. The vibrational and rotational transitions may be coupled, i.e., simultaneous changes in vibrational and rotational quanta may occur in a single collision. The rates of such transitions are even less known. In addition, calculation of the bound-free transition processes are made complicated because of the existence of the rotational barrier. Experiments are equally difficult for the high states because the radiation emission, absorption, scattering, or fluorescence of the upper states, if they exist, are usually weak for those states.

It is the purpose of the present work to estimate the excess energy contained in the high vibrational and rotational states in an expanding reacting flow. The work is based on the assumption that the population distribution of the vibrational and rotational states, when normalized by their Boltzmann values, is describable by a polynomial in energy coordinates containing seven parameters. The parameters are determined by invoking seven known physical constraints. They are, one at the ground state, three at the dissociation limit, the mass conservation law, the Treanor distribution for the intermediate states, and the requirement that the method results in a most conservative estimate of the excitation energy. This procedure circumvents having to know the state-to-state transition rates. The calculation is performed for N_2, O_2, NO, CO, and H_2, and the results are packaged into a group of numbers, from which the excess energy can be determined through interpolation. In order to assess how large the excess energy is, and how this phenomenon affects the thermodynamic state in a high enthalpy wind tunnel flow, calculation is made of the flows including the excess excitation phenomenon for typical shock-tunnel conditions. The calculation shows that the excess energy is a significant fraction of the total enthalpy of the flow.

An effort similar to this was made in the work of Ruffin,[13] wherein the average vibrational temperature representing the vibrational energy T_{vav} is calculated, as well as the vibrational temperature characterizing the low vibrational states T_v. The work shows that T_{vav} is always higher than T_v, the difference representing the excess vibrational energy. The present work is an improvement over that work in that the effect of atomic recombination into the high levels, which was neglected by Ruffin, and the energy contained in the excited rotational states are both accounted for.

Until recently, there existed another issue with the expanding diatomic gas flows that, in experimental observations, vibrational relaxation seemingly proceeds at a rate faster[17,18] than that expected from the known vibrational relaxation times.[19] However, in a recent experiment conducted in a clean environment, such anomaly did not occur.[20,21] Therefore, this problem is not addressed in the present work.

Derivation

Fundamentals of Molecular Relaxation

Imagine a reacting system in which a molecular species M coexists with the atomic species A and B that are produced as a result of its dissociation:

$$M \rightleftharpoons A + B$$

Only the ground electronic state of the molecule is considered here. In a nonequilibrium environment, the populations of the vibrational and rotational states of such a molecular species are governed by a master equation that is well known (see, e.g., Chap. 3 of Ref. 1). By defining the equilibrium number density $n_E(v, J)$ by

$$n_E(v, J) = n_A n_B \frac{Q(v, J)}{Q_A Q_B} \exp\left[\frac{D - E(v, J)}{T}\right] \tag{4}$$

and the normalized nonequilibrium population $\rho(v, J)$ by

$$\rho(v, J) = \frac{n(v, J)}{n_E(v, J)} \tag{5}$$

the master equation can be written as (see Chap. 3 of Ref. 1)

$$\frac{1}{n_x}\frac{\partial \rho(v, J)}{\partial t} = \sum_{J'}\sum_{v'} K(J, v, J', v')[\rho(v', J') - \rho(v, J)] + K(J, v, c)[1 - \rho(v, J)] \tag{6}$$

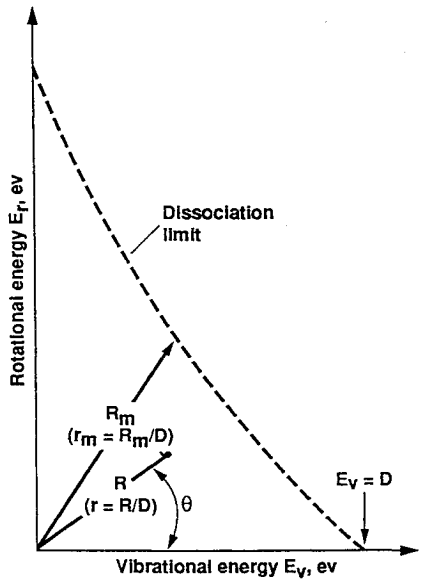

Fig. 1 Polar coordinate description of vibration-rotation space.

If the collision energy kT is larger than the energy gaps between the neighboring states, one can consider the states to be continuously distributed. Then, using the notation

$$v' = v + \Delta v, \qquad J' = J + \Delta J$$

Eq. (6) can be written as

$$\frac{1}{n_x}\frac{\partial \rho}{\partial t} = \int\int K(J, v, J', v')[\rho(v', J') - \rho(v, J)]\Omega \Delta v \Delta J + K(J, v, c)[1 - \rho(v, J)] \tag{7}$$

The quantity Ω is the scale factor associated with the transformation of the coordinates from the discrete to the continuum type. Among the low vibrational and rotational states, it is known that the transitions occur preferentially among the neighboring states, i.e., a selection rule exists. For these states, the second moment of transition defined by

$$M = \int\int K(J, v, J', v')(\Delta v J)^2 \Omega \, \mathrm{d}(\Delta v) \, \mathrm{d}(\Delta J) \tag{8}$$

is bounded. Here, the quantity ΔvJ symbolically represents the distance between the (v', J') and the (v, J) points in the v-J coordinate system. In that case, the master equation can be written further as (see Chap. 3 of Ref. 1)

$$\frac{1}{n_x}\frac{\partial \rho}{\partial t} = \nabla(M \nabla \rho) + K(v, J, c)(1 - \rho)$$

where the sign ∇ represents a two-dimensional derivative in the v and J coordinates. For the low states, the rate coefficient $K(v, J, c)$ is small because the threshold energy $\Delta E = D - E(v, J)$ is large for those states. Therefore, the last equation can be written for these states approximately as (among low states)

$$\frac{1}{n_x}\frac{\partial \rho}{\partial t} \approx \nabla(M \nabla \rho) \tag{9}$$

which is a diffusion equation

To describe the behavior of the normalized population ρ in the two-dimensional space of v and J, one introduces polar coordinates r and θ shown in Fig. 1. R and r are first defined as

$$R = \sqrt{E_v^2 + E_r^2}, \quad \text{eV} \tag{10}$$

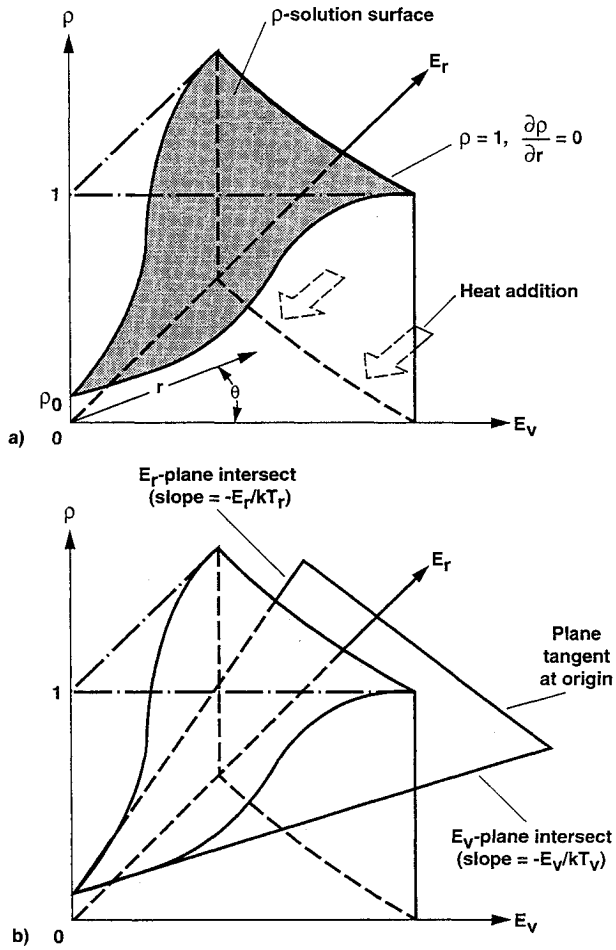

Fig. 2 Mathematical behavior of the solution of the master equation in the E_v-E_r-ρ space.

$$r = R/D \tag{11}$$

θ is defined by

$$\theta = \tan^{-1}(E_r/E_v) \tag{12}$$

The dissociation limit is given by $R = R_m(\theta)$ or $r = r_m(\theta)$.

Behavior at Origin

The solution of the master Eq. (7) forms, in general, a surface in the v-J-ρ or r-θ-ρ coordinate system. The surface is illustrated in Fig. 2a. The problem resembles that of a triangular-shaped piece of heat conductor heated at the hypotenuse. At the origin, the piece is in contact with a heat sink. Since the equation resembles a diffusion equation at and near the origin $E_v = E_r = 0$, and since the solution of a diffusion equation around a point is a plane, there exists a plane tangent to the solution at the origin, as illustrated in Fig. 2b. The slope of the E_v-plane intersect of the tangent plane must be compatible with the given vibrational temperature, because vibrational temperature is defined as the ratio of the populations between the excited and the ground vibrational states for $J = 0$, i.e.,

$$[n(v)/n(0)] = \exp[-E(v)/kT_v]$$

By normalizing $n(v)$ by the equilibrium value corresponding to T, one obtains the relation

$$D\left(\frac{\partial \rho}{\partial E_v}\right)_0 = \rho_0\left(-\frac{D}{kT_v} + \frac{D}{kT}\right)$$

For convenience, the quantity on the right side is designated by

$$\delta T_v = -\frac{D}{kT_v} + \frac{D}{kT} \tag{13}$$

so that

$$D\left(\frac{\partial \rho}{\partial E_v}\right)_0 = \rho_0 \delta T_v \tag{14}$$

Likewise, for the E_r-plane intersect, there results

$$D\left(\frac{\partial \rho}{\partial E_r}\right)_0 = \rho_0 \delta T_r \tag{15}$$

where

$$\delta T_r = -\frac{D}{kT_r} + \frac{D}{kT} \tag{16}$$

In an expanding flow through a nozzle, the flow residence time is usually such that rotational temperature equalizes with the translational temperature, so that

$$\delta T_r = 0 \tag{17}$$

In this coordinate system, the two conditions at the origin, Eqs. (14) and (15), and the condition that the solution is a plane at the origin, can be combined into a single equation

$$\left(\frac{\partial \rho}{\partial r}\right)_0 = \rho_0(\delta T_r \sin\theta + \delta T_v \cos\theta) = \rho_0 \delta T_v \cos\theta \tag{18}$$

Behavior at Dissociation Limit

Among the high vibrational and rotational states, the quantity M in Eq. (8) is not bounded. Therefore, one must study the integro-differential Eq. (7) to understand the behavior among these states. Among these states, all transitions, for both bound-bound and bound-free, occur approximately with a fixed cross section. If the variation of r_m with θ (from 1 at $\theta = 0$ to about 2 at $\theta = \pi/2$) can be ignored and can be assumed to remain unity for all θ, then ρ becomes a function only of r. Equation (7) for these upper states can then be written as

$$\frac{1}{n_x}\frac{\partial \rho}{\partial t} = \int_0^{r_m} K(r, r')(\rho' - \rho)\, dr' + K(r, c)(1 - \rho)$$
$$r_m - r << 1 \tag{19}$$

where ρ' represents $\rho(v')$. This equation is similar to that derived by Brau.[7]

Designating the transition cross section by σ and the mean thermal speed by $\bar{v}$, and introducing the symbol $\alpha = kT/D$, $K(r, c)$ can be written as

$$K(r, c) = \sigma\bar{v}\int_0^1 \exp\left(-\frac{1 - r + r'}{\alpha}\right) dr'$$
$$= \sigma\bar{v}\alpha \exp\left(-\frac{1 - r}{\alpha}\right), \quad \text{m}^3/\text{s} \tag{20}$$

Likewise, $K(r, r')$ becomes

$$K(r, r') = \sigma\bar{v}\alpha, \quad \text{m}^3/\text{s} \quad \text{for} \quad r' \le r \tag{21}$$

$$K(r, r') = \sigma\bar{v}\alpha \exp\left(-\frac{r' - r}{\alpha}\right), \quad \text{m}^3/\text{s} \quad \text{for} \quad r' \ge r \tag{22}$$

Among these high states, a quasi-steady-state exists,[5,9,10] and so the left side of Eq. (19) can be set to zero, leading to

$$\int_0^1 K(r, r')(\rho' - \rho)\, dr' + K(r, c)(1 - \rho) \approx 0$$
$$r_m - r << 1 \tag{23}$$

Eq. (23) can be written as

$$\rho = \int_0^1 G(r, r')\rho'\, dr' + H(r, c), \qquad r_m - r << 1 \tag{24}$$

where

$$G(r, r') = \frac{K(r, r')}{\int_0^{r_m} K(r, r'')\, dr'' + K(r, c)}$$

$$H(r, c) = \frac{K(r, c)}{\int_0^{r_m} K(r, r'')\, dr'' + K(r, c)}$$

Equation (24) is a linear integral equation of Fredholm type of the second kind. It can be solved approximately in the region $r_m - r << 1$, by expanding the exponential function in Eqs. (20) and (22) into a Taylor series around the point $r = r_m$. The resulting equation can be solved by using the method of successive substitution. With the assumption of $\rho_0 = 0$, the first two terms of the solution to Eq. (24) become

$$\rho = 1 - 0.25[(r_m - r)^2]/\alpha + 0[(r_m - r)^3]$$

This means that the value of ρ is unity at the dissociation limit

$$\rho(r_m) = 1 \tag{25}$$

the slope is zero at the dissociation limit

$$\left(\frac{\partial \rho}{\partial r}\right)_{r_m} = 0 \tag{26}$$

and the curvature at the dissociation limit is

$$\left(\frac{\partial^2 \rho}{\partial r^2}\right)_{r_m} = -0.5\,\frac{D}{kT} \tag{27}$$

The relations (25) and (26) had been observed empirically in Refs. 5 and 9–11. The relation (26) is used also by Ruffin in his approximate model.[13] The present derivation reaffirms those observations. The condition (27) is an additional relationship obtained through the present analysis.

Behavior Among Intermediate Levels

In an environment where molecule-to-molecule collisions dominate over atom-to-molecule collisions, the low-intermediate states attain the so-called Treanor distribution of population described by[2]

$$n_v = \frac{n_M}{Q_M}\exp\left[-v\left(\frac{\omega_e}{kT_v} - \frac{\omega_e}{kT}\right) - \frac{E_v}{kT}\right]$$

In the notations of the present work, it becomes

$$\rho_v = \rho_0 \exp\left\{-\left[\frac{E_v}{D} + \frac{\omega_e x_e}{D}\left(\frac{E_v}{\omega_e}\right)^2\right]\left(\frac{D}{kT_v} - \frac{D}{kT}\right)\right\}$$

or

$$\ell\!\!\ell(\rho_v) = \ell\!\!\ell(\rho_0) + \delta T_v r + \delta T_v \left(\frac{\omega_e x_e}{D}\right)\left(\frac{D}{\omega_e}\right)^2 r^2 \quad (28)$$

Polynomial Model

The solution of the master Eq. (6) in the r-θ coordinate system is assumed in the present work to be expressible in the form

$$\ell\!\!\ell[\rho(r, \theta)] = a_0 + a_1(\theta)r + a_2(\theta)r^2 + a_3(\theta)r^m + a_4(\theta)r^n \quad (29)$$

The average energy ε is given in this case as

$$\varepsilon = \frac{\sum\sum \exp[a_1 r + a_2 r^2 + a_3 r^m + a_4 r^n - E/kT]Eg}{\sum\sum \exp[a_1 r + a_2 r^2 + a_3 r^m + a_4 r^n - E/kT]g} \quad (30)$$

The coefficients a_i and the exponents m and n are determined by imposing the following constraints:

Slope at the Origin

To satisfy Eq. (18), there follows

$$a_1(\theta) = \delta T_v \cos\theta + \delta T_r \sin\theta = \delta T_v \cos\theta \quad (31)$$

Treanor Distribution Among Intermediate States

By comparing the r^2 term in Eq. (29) with that in Eq. (28), there follows

$$a_2 = \delta T_v(\omega_e x_e/D)(D/\omega_e)^2 \quad (32)$$

Imposition of this condition tacitly assumes that molecule-to-molecule collisions dominate over atom-to-molecule collisions, which will be true provided the degree of dissociation is not large.

Value at the Dissociation Limit

To satisfy Eq. (25), there follows

$$\ell\!\!\ell[\rho(r_m)] = a_0 + a_1(\theta)r_m + a_2(\theta)r_m^2 + a_3(\theta)r_m^m + a_4(\theta)r_m^n = 0 \quad (33)$$

Slope at the Dissociation Limit

To satisfy Eq. (26), there follows

$$\left(\frac{1}{\rho}\frac{\partial\rho}{\partial r}\right)_{r_m} = a_1(\theta) + 2a_2(\theta)r_m + ma_3(\theta)r_m^{m-1} + na_4(\theta)r_m^{n-1} = 0 \quad (34)$$

Solving Eqs. (33) and (34) for a_3 and a_4, one obtains

$$a_3 = -\frac{na_0 + (n-1)a_1 r_m + (n-2)a_2 r_m^2}{(n-m)r_m^m} \quad (35)$$

$$a_4 = -\frac{a_0 + a_1 r_m + a_2 r_m^2 + a_3 r_m^m}{r_m^n} \quad (36)$$

Curvature at the Dissociation Limit

The quantity $\ell\!\!\ell\,\rho$ varies from a_0, a value of the order of -100, to zero, whereas ρ varies from $\exp(a_0)$, a near-zero value, to unity. Therefore, in applying the condition on curvature, Eq. (27), the vertical scale must be stretched by the absolute value of a_0, leading to

$$\frac{\partial^2}{\partial r^2}(\ell\!\!\ell\,\rho)_{r_m} = 2a_2 + m(m-1)a_3 r_m^{m-2} + n(n-1)a_4 r_m^{n-1} \approx -0.5|a_0|\frac{D}{kT} \quad (37)$$

Mass Conservation

The mass conservation law dictates that the sum of all internal state populations must equal the known total number density of the molecule n_M, i.e.,

$$\sum_v \sum_J n(v, J) = \sum_v \sum_J \rho(v, J) n_E(v, J) = n_M, \quad \mathrm{m}^{-3}$$

One can introduce the normalized nonequilibrium molecular density ρ_M, which is the ratio between the given number density and the equilibrium value based on the free-state densities

$$\rho_M = \frac{n_M}{n_{EM}} = \frac{n_M}{n_A n_B}\frac{Q_A Q_B}{Q_M}\exp\left(-\frac{D}{kT}\right) \quad (38)$$

The mass conservation condition can then be expressed as

$$\rho_M = \frac{1}{Q_M}\sum_\theta\sum_r \rho(r, \theta)g\exp(-E/kT) = \frac{\rho_0}{Q_M}\sum_\theta\sum_r \exp[a_1(\theta)r + a_2(\theta)r^2 + a_3(\theta)r^m + a_4(\theta)r^n]g\exp(-E/kT) \quad (39)$$

Most Conservative Estimation

The choice of parameters should be such that the excitation energy deduced is most conservative, i.e., the least. The excitation energy content along a fixed θ can be defined as

$$\varepsilon_\theta = \int_0^{r_m} E(r, \theta)\rho(r, \theta)n_E(r, \theta)\,dr \quad (40)$$

Taking n as the parameter to be adjusted for this purpose, the condition can be written as

$$\frac{\partial\varepsilon_\theta}{\partial n} = 0 \quad (41)$$

By solving Eqs. (35–37) and (41), one can, in principle, determine a_3, a_4, m, and n, uniquely. However, it is prohibitively expensive to do so. Hence, calculation is made here of the curvature, $(\partial^2\,\ell\!\!\ell\,\rho/\partial r^2)_{r_m}$ [to see if the condition Eq. (37) is met], and the energy ε_θ [to see if the condition Eq. (41) is met], for a range of m and n values, with the a_3 and a_4 values constrained by Eqs. (35) and (36). The results show that both the curvature and the energy content are a weak function of m and n. When m is fixed as 4, the n value that satisfies Eq. (37) varies between 5–8. Therefore, for simplicity, m and n values are fixed as

$$m = 4, \qquad n = 6 \quad (42)$$

Typical behavior of the normalized population ρ so-determined is shown in Fig. 3. The figure confirms the qualitative description given in Fig. 2.

For given values of ρ_0, T, and T_v, Eqs. (35), (36), (39), (30), and (3) are evaluated for the m and n values given by Eq. (42). The resulting E_x values are then regarded as a function of ρ_M, T, and T_v. The calculations are carried out for 15 values of ρ_M, and five values each of T and T_v. The variation of E_x with T and T_v are expressed using a fourth-order poly-

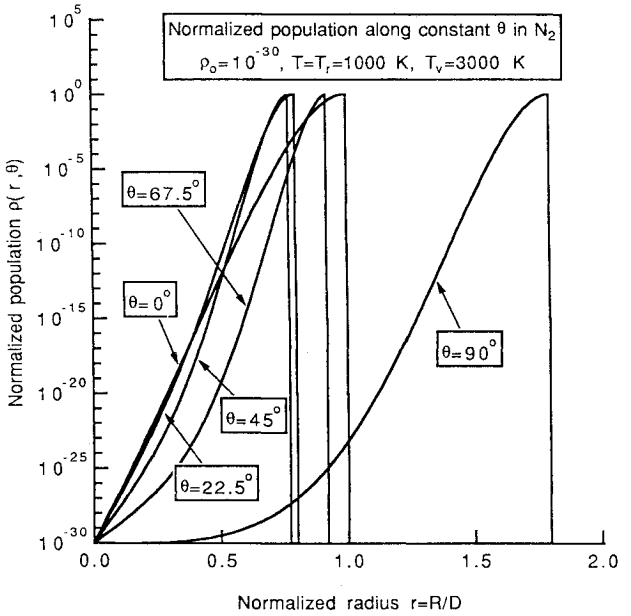

Fig. 3 Variation of normalized population ρ with r and θ for a typical flow condition for N_2.

nomial. The resulting $15 \times 5 \times 5 = 375$ values are presented for use in determining E_x through interpolation. The source program of the interpolating subroutine is given in Ref. 22. The calculation has been carried out for N_2, O_2, NO, CO, and H_2. The coefficient values, which are different from those in Ref. 22, are available on request.

Comparison with Other Works

Ruffin's Theoretical Calculation

In order to verify the validity of the present procedure for determining the distribution of internal states, the calculated vibrational distributions are compared first with those obtained by Ruffin.[13] The cases considered are those of N_2 cooling from 6000 to 1000 K, with an assumed average vibrational temperature of 2500 or 5800 K. The average vibrational temperature is defined by Ruffin as the temperature that corresponds to the vibrational energy contained. The vibrational temperature defined by the two lowest levels, which is the vibrational temperature used in the present work, is 2460 and 4610 K, respectively. For both cases, quasi-steady-state distribution is calculated by Ruffin through integration of master equation. The calculation does not account for atomic recombination into the upper levels, and therefore, the condition Eq. (25) is not enforced. For the purpose of comparison, the exponents m and n are varied over a range.

The results of the present calculation are presented in Figs. 4a and 4b, and compared with the calculations of Ruffin. For the case shown in Fig. 4a, the present calculations lead to much higher populations than the Ruffin's values for levels above 60,000 cm^{-1}. This is because of the suspension of Eq. (25) in Ruffin's calculation. Except for the case with $m = 3$ and $n = 4$, the present results are generally in agreement with Ruffin's work below 60,000 cm^{-1}. For the case in Fig. 4b, the populations of the upper levels calculated by the present method are not much different from those of Ruffin. Apparently, at the high vibrational temperature, suspension of Eq. (25) does not lead to a large error. Here, the choice of $m = 4$ and $n = 6$ is seen to give the closest agreement with Ruffin's calculation below 60,000 cm^{-1}. Note that the concave-upward trend of the Treanor distribution is reproduced by both the present and Ruffin's calculations for both cases.

Bender Experiment

Secondly, the present method is compared with the experimental data of Bender, in which the population of first 10

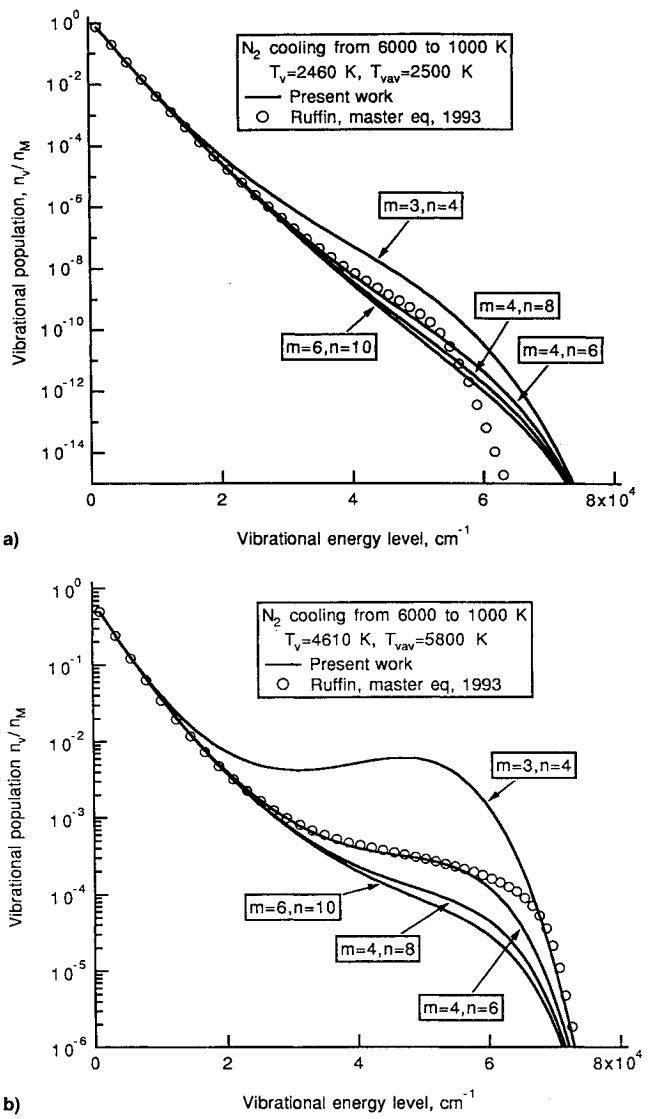

Fig. 4 Comparison between the present method and master equation integration by Ruffin[13] for N_2; original temperature = 6000 K, pressure = 1 atm, cooled translational temperature = 1000 K: a) T_v = 2460 K (T_{vav} = 2500 K) and b) T_v = 4610 K (T_{vav} = 5800 K).

vibrational levels of CO are measured in an arcjet wind-tunnel nozzle flow of an Ar-CO mixture.[14] The case compared is one in which the CO fraction was 9.3% by volume, and settling chamber temperature was 2400 K. The m and n values of 4 and 6 are used for this purpose. The results are compared with the experimental data and the result of the calculation of Ruffin[13] in Fig. 5. Two different methods have been used by Ruffin: 1) master equation integration and 2) a simplified model. As seen in the figure, the present method agrees with both the experimental data and Ruffin's calculations for the observed range of vibrational levels. The difference between the present result and the result of Ruffin for higher vibrational levels is attributed also to the suspension of Eq. (25) in Ruffin's work. The Treanor distribution observed experimentally is correctly reproduced by both the present method and Ruffin's work, even though argon constitutes 91% of the flow. This supports imposition of Treanor distribution [Eq. (32)].

Horn and Oettinger Experiment

Next, the present method is compared with the experimental data of Horn and Oettinger.[15] In that experiment, a subsonic flow in a tube was heated with a microwave discharge. The measurement was made in the flow in the downstream relaxation region. The test gas was a mixture of CO

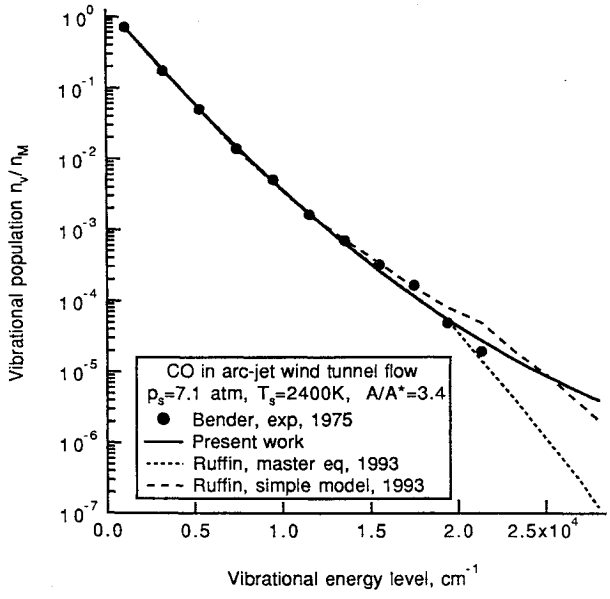

Fig. 5 Comparison between the present method and Ruffin's results for the experimental condition of Bender[14] for CO in an arcjet wind-tunnel nozzle.

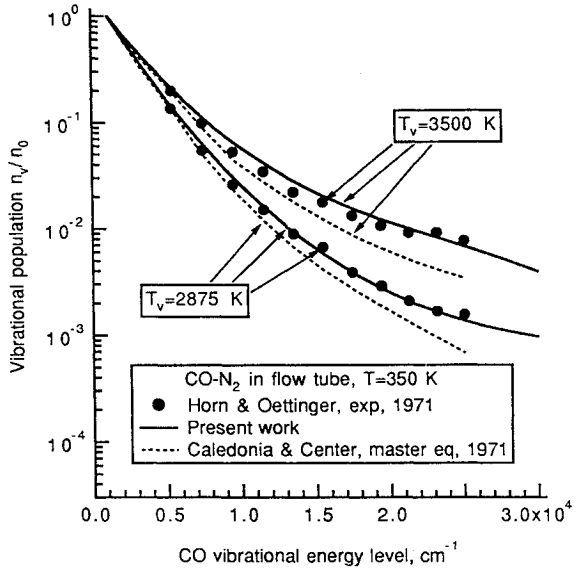

Fig. 6 Comparison between the present method and the results of Caledonia and Center[6] for the experimental conditions of Horn and Oettinger[15] for CO-N_2 in microwave-heated flow in a tube.

and N_2. Two test conditions are reported in Ref. 15: one for T_v = 2875 K, and the other T_v = 3500 K. For this case, ρ_M values are not known. Therefore, ρ_M is adjusted in the present calculation until the best match with the experimental data is obtained: to 3×10^{-63} to the case of T_v = 2875 K and 1×10^{-55} for the case of T_v = 3500 K. The values of m and n are kept at 4 and 6, respectively. In Fig. 6, the results of the present calculation are compared with the experimental data. Shown also in the figure are the results of the master equation calculation by Caledonia and Center.[6] As seen in the figure, the present method can reproduce the data closely, and at least as well as the work of Caledonia and Center.

Joekle and Peyron Experiment

Lastly, the present method is compared with the experimental data of Joekle and Peyron.[16] The experimental method used was the same as that of Horn and Oettinger. The parameters selected are: $\rho_M = 3 \times 10^{-63}$, m = 4, and n = 6, respectively. The present method is compared with the experimental data and the master equation calculation by Caledonia and Center[6] in Fig. 7. The two curves attributed to Caledonia and Center were obtained using different parameters in the calculation. Again, the present method is in agreement with the experimental data and the master equation calculation.

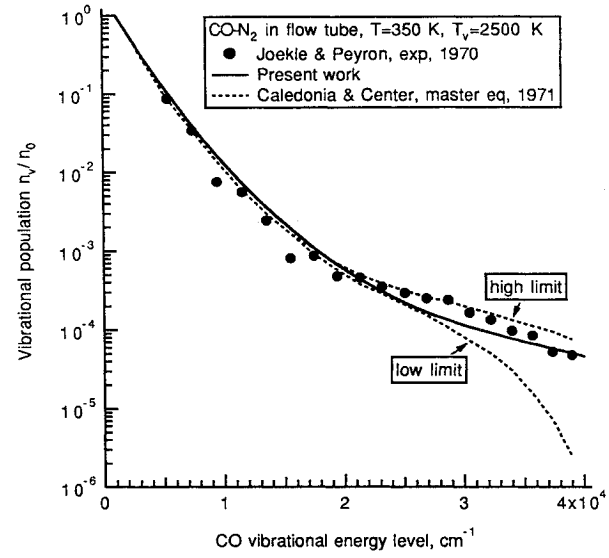

Fig. 7 Comparison between the present method and results of Caledonia and Center[6] for the experimental conditions of Joekle and Peyron[16] for CO-N_2 in microwave-heated flow in a tube.

Application

Following the procedure described above, the excess energy E_x is calculated for typical shock-tunnel flow conditions. In this flow, N_2 at p_s = 100 atm in a settling chamber is expanded through a contoured nozzle of a length of 3 m and an area ratio of 200. The flow enthalpy is varied between 7.5–25 MJ/kg in the calculation. The calculation of E_x is carried out fully-coupled with fluid motion using the NOZNT code.[23] For the purpose of comparison, the calculation is carried out also excluding E_x. The calculation is not performed for enthalpies below 7.5 MJ/kg, because the NOZNT code requires the presence of a significant amount of electrons in the flow.

The results of the calculation are shown in Figs. 8 and 9. In Fig. 8a, the translational-rotational temperature T and the vibrational temperature T_v along the nozzle are compared for the cases with and without E_x. As seen here, T is significantly lower when E_x is included. In Fig. 8b, the flow velocity and the magnitude of E_x, normalized by the flow enthalpy H, are shown. As seen here, velocity is about 1% slower for the case with finite E_x (4978 vs 5027 m/s). The excess energy E_x reaches 3% of the flow enthalpy for this case. Although not shown, most of this excess energy is in the vibrational mode: the energy contained in the highly excited rotational states is found to be negligibly small.

In Fig. 9, E_x/H and the fractional decrement of flow velocity at the nozzle exit $-\Delta V/V$, where ΔV is the difference between the velocity with and without E_x, and V in the denominator is the velocity without E_x, are plotted against the flow enthalpy. As seen here, both these quantities are larger at low enthalpies, at least within the range calculated. Presumably, E_x approaches zero below 7.5 MJ/kg. The ratio E_x/H exceeds 6%, and $-\Delta V/V$ exceeds 3% at 7.5 MJ/kg. This shows that the excess excitation energy must be accounted for in the calculation of properties in a high-enthalpy nozzle flow, especially in a weakly dissociated regime.

Discussion

Although the present method incorporates and accommodates many existing theories and experimental data, sev-

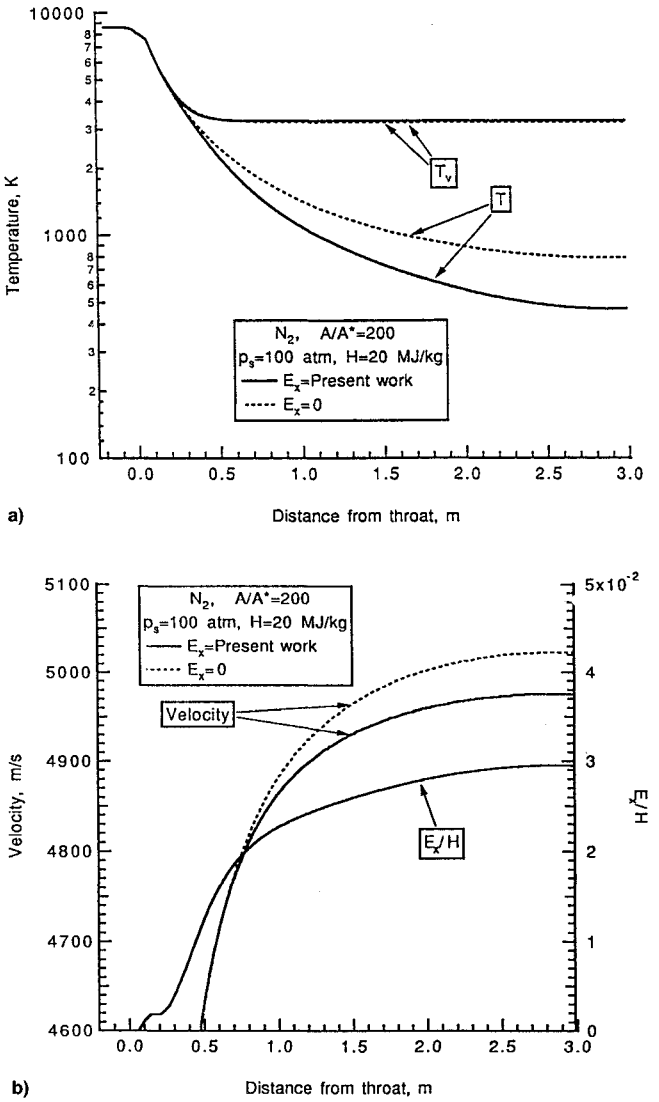

Fig. 8 Effect of excess excitation energy on shock-tunnel nozzle flow of nitrogen; nozzle length = 3 m, exit area ratio = 200, p_s = 100 atm, H = 20 MJ/kg: a) translational-rotational and vibrational temperatures and b) E_x/H and V.

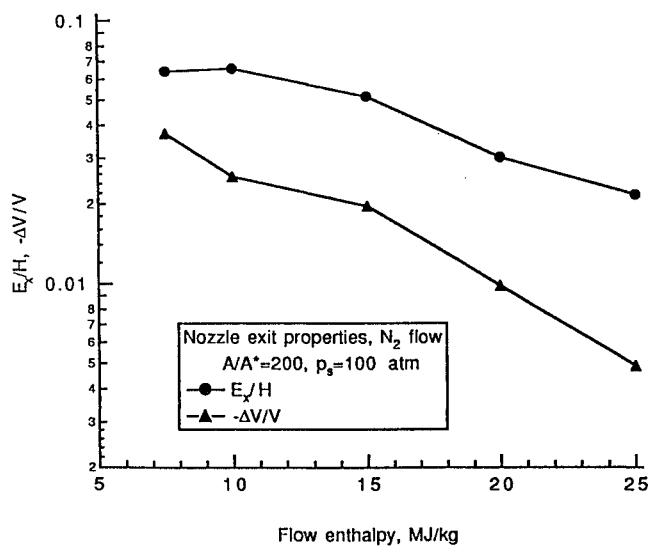

Fig. 9 Variation of E_x/H and velocity decrement $-\Delta V/V$ with enthalpy for nitrogen flow; nozzle length = 3 m, exit area ratio = 200, p_s = 100 atm.

eral problems still remain. First, there is an uncertainty about the values of m and n. As mentioned in polynomial method, one must solve Eqs. (37) and (41) simultaneously to determine these parameters precisely, which is prohibitively expensive to do. The two quantities are functions of T_v, ρ_M, and D/kT. Finding the functional relationship between the values of m and n and the three parameters is left for the future.

In assessing the impact of the present work on the behavior of an expanding flow (see Figs. 8 and 9), the NOZNT code[23] was used. In that code, Millikan and White-type relaxation is assumed to occur to the vibrational energy of a harmonic oscillator with a temperature corresponding to the lowest two states. According to Ruffin,[13] Millikan and White-type vibrational relaxation occurs with respect to the average vibrational energy, which means that the sum of the vibrational energy calculated in NOZNT and the excess energy defined in the present work relaxes according to the Millikan and White formula. This point needs to be resolved in the future also.

Finally, it is noted that the results of the past experiments, in which the vibrational temperature was measured indirectly using either the sodium (or chromium) resonance line absorption technique (see, e.g., Ref. 24), langmuir probes, or microwave devices,[25-27] have not yet been fully explained either by the experimental work of Sharma et al.,[20,21] the theoretical work of Ruffin,[13] or the present work. In general, those experimental data show vibrational temperatures lower than predicted by the latest theories.

Conclusions

The energy contained in the high vibrational and rotational states of a diatomic molecule in a nonequilibrium thermochemical state during expansion is estimated using an assumption that the internal state populations, when normalized by their respective equilibrium values, are describable by a polynomial. The population distributions so-determined agree with the existing experimental data and calculations. For a typical flow in a shock-tunnel nozzle, the energy contained in the high states reaches up to 6% of the total enthalpy of the flow, and the flow velocity is reduced by up to about 3%. Several problems still remain to be resolved in the future.

Acknowledgments

The author wishes to express sincere thanks to Yen Liu and Marcel Vinokur of Ames Research Center, Moffett Field, California, for providing the computer code for determination of vibrational and rotational levels. Thanks are due also to Stephen Ruffin of the Georgia Institute of Technology, Atlanta, Georgia, who provided the computer code for the reproduction of his earlier work.

References

[1]Park, C., *Nonequilibrium Hypersonic Aerothermodynamics*, Wiley, New York, 1990.

[2]Treanor, C. E., Rich, J. W., and Rohm, R. G., "Vibrational Relaxation of Anharmonic Oscillators with Exchange-Dominated Collisions," *Journal of Chemical Physics*, Vol. 48, No. 4, 1968, pp. 1798–1807.

[3]Rich, J. W., and Rohm, R. G., "Population Distribution During Vibrational Relaxation of Diatomic Gas," *Proceedings of the 11th Symposium (International) on Combustion*, The Combustion Inst., Pittsburgh, PA, 1967, pp. 240–243.

[4]Bray, K. N. C., "Vibrational Relaxation of Anharmonic Oscillator Molecules: Relaxation Under Isothermal Conditions," *Proceedings of the Physical Society: Journal of Physics B*, Vol. 1, No. 4, 1968, pp. 705–717.

[5]Bray, K. N. C., and Pratt, N. H., "Conditions for Significant Gasdynamically Induced Vibration-Recombination Coupling," *Proceedings of the 11th Symposium (International) on Combustion*, The Combustion Inst., Pittsburgh, PA, 1967, pp. 23–36.

[6]Caledonia, G. E., and Center, R. E., "Vibrational Distribution Function in Anharmonic Oscillators," *Journal of Chemical Physics*, Vol. 55, No. 2, 1971, pp. 552–561.

[7]Brau, C. A., "Classical Theory of Vibrational Relaxation of Anharmonic Oscillators," *Physica*, Vol. 58, No. 4, 1972, pp. 533–553.

[8]Flament, C., "Dissociation-Vibration Coupling Application to Hypersonic Nozzle Flows," *La Recherche Aerospatiale*, Vol. 1991, No. 2, 1991, pp. 67–78.

[9]Sharma, S. P., Huo, W. M., and Park, C., "The Rate Parameters for Coupled Vibration-Dissociation in a Generalized SSH Approximation," *Journal of Thermophysics and Heat Transfer*, Vol. 6, No. 1, 1992, pp. 9–21.

[10]Landrum, D. B., and Candler, G. V., "Vibration-Dissociation Coupling in Nonequilibrium Flows," AIAA Paper 91-0466, Jan. 1991.

[11]Sharma, S. P., and Schwenke, D. W., "The Rate Parameters for Coupled Rotation-Vibration-Dissociation Phenomenon in H_2," *Journal of Thermophysics and Heat Transfer*, Vol. 5, No. 4, 1991, pp. 469–480.

[12]Ruffin, S. M., and Park, C., "Vibrational Relaxation of Anharmonic Oscillators in Expanding Flows," AIAA Paper 92-0806, Jan. 1992.

[13]Ruffin, S. M., "Vibrational Energy Transfer of Diatomic Gases in Hypersonic Expanding Flows," Ph.D. Dissertation, Dept. of Aeronautics and Astronautics, Stanford Univ., Stanford, CA, June 1993.

[14]Bender, D. J., "Measurement of Vibrational Population Distribution in a Supersonic Expansion of Carbon Monoxide," Ph.D. Dissertation, Dept. of Mechanical Engineering, Stanford Univ., Stanford, CA, March 1975.

[15]Horn, K. P., and Oettinger, P. E., "Vibrational Energy Transfer in Diatomic Gas Mixtures," *Journal of Chemical Physics*, Vol. 54, No. 7, 1971, pp. 3040–3046.

[16]Joekle, R., and Peyron, M., "Infrared Chemiluminescence of Carbon Monoxide Excited by Activated Nitrogen," *Journel de Chimie Physique et de Physicochimie Biologique*, Vol. 67, No. 6, 1970, pp. 1175–1181.

[17]Hurle, I. R., "Nonequilibrium Flows with Special Reference to the Nozzle Flow Problem," *Proceedings of the 8th International Shock Tube Symposium*, Chapman and Hall, London, 1971, pp. 3/1–3/37.

[18]Blom, A. P., Bray, K. N. C., and Pratt, N. H., "Rapid Vibrational De-Excitation Influenced by Gasdynamic Coupling," *Astronautica Acta*, Vol. 15, Nos. 5 and 6, 1970, pp. 487–494.

[19]Millikan, R. C., and White, D. R., "Systematics of Vibrational Relaxation," *Journal of Chemical Physics*, Vol. 39, No. 12, 1963, pp. 3209–3213.

[20]Sharma, S. P., Ruffin, S. M., Gillespie, W. D., and Meyer, S. A., "Vibrational Relaxation Measurements in an Expanding Flow Using Spontaneous Raman Scattering," *Journal of Thermophysics and Heat Transfer*, Vol. 7, No. 4, 1993, pp. 697–703.

[21]Gillespie, W. D., Bershader, D., Sharma, S., and Ruffin, S. M., "Raman Scattering Measurements of Vibrational and Rotational Distribution in Expanding Nitrogen," AIAA Paper 93-0274, Jan. 1993.

[22]Park, C., "Estimation of Excitation Energy of Diatomic Molecules in Expanding Nonequilibrium Flows," AIAA Paper 92-0805, Jan. 1992.

[23]Park, C., and Lee, S. H., "Validation of Multitemperature Nozzle Flow Code," *Journal of Thermophysics and Heat Transfer*, Vol. 9, No. 1, 1995, pp. 9–16.

[24]Hurle, I. R., Russo, A. L., and Hall, J. G., "Spectroscopic Studies of Vibrational Nonequilibrium in Supersonic Nozzle Flows," *Journal of Chemical Physics*, Vol. 40, No. 8, 1964, pp. 2076–2089.

[25]Dunn, M. G., and Lordi, J. A., "Measurement of Electron Temperature and Number Density in Shock Tunnel Flows, Part 2. $NO^+ + e$ Dissociative Recombination Rate in Air," *AIAA Journal*, Vol. 7, No. 11, 1969, pp. 2099–2104.

[26]Dunn, M. G., and Lordi, J. A., "Measurement of $N_2^+ + e$ Dissociative Recombination in Expanding Nitrogen Flows," *AIAA Journal*, Vol. 8, No. 2, 1970, pp. 339–345.

[27]Dunn, M. G., and Lordi, J. A., "Measurement of $O_2^+ + e$ Dissociative Recombination in Expanding Oxygen Flows," *AIAA Journal*, Vol. 8, No. 4, 1970, pp. 614–618.